sciendo

TRANSACTIONS ON AEROSPACE RESEARCH
4(257) 2019, pp.32-45
DOI: 10.2478/tar-2019-0021
eISSN 2545-2835

CFD APPROACH TO MODELLING HYDRODYNAMIC CHARACTERISTICS OF UNDERWATER GLIDER

Kamila Stryczniewicz
Warsaw University of Technology,
Department of Aerodynamics, Institute of Aeronautics and Applied Mechanics,
Nowowiejska 24, 00-665 Warsaw, Poland
kgra@meil.pw.edu.pl

Przemysław Drężek
Research Network Łukasiewicz – Institute of Aviation,
Department of Aerodynamics,
Al. Krakowska 110/114, 02-256 Warsaw, Poland
przemyslaw.drezek@ilot.edu.pl

Abstract

Autonomous underwater gliders are buoyancy propelled vehicles. Their way of propulsion relies upon changing their buoyancy with internal pumping systems enabling them up and down motions, and their forward gliding motions are generated by hydrodynamic lift forces exerted on a pair of wings attached to a glider hull. In this study lift and drag characteristics of a glider were performed using Computational Fluid Dynamics (CFD) approach and results were compared with the literature. Flow behavior, lift and drag forces distribution at different angles of attack were studied for Reynolds numbers varying around 10^5 for NACA0012 wing configurations. The variable of the glider was the angle of attack, the velocity was constant. Flow velocity was 0.5 m/s and angle of the body varying from –8° to 8° in steps of 2°. Results from the CFD constituted the basis for the calculation the equations of motions of glider in the vertical plane. Therefore, vehicle motion simulation was achieved through numeric integration of the equations of motion. The equations of motions will be solved in the MatLab software. This work will contribute to dynamic modelling and three-dimensional motion simulation of a torpedo shaped underwater glider.

Keywords: AUV, CFD, drag, glider, underwater glider.

1. INTRODUCTION

The starting point and inspiration to this work are intensive research that goes on in the area of dynamics modelling of underwater vehicles, their maneuverability and performance, driven by their increasing applications in oceanography, military, natural environment safety.

The research objective was to study general dynamics model of an underwater vehicle with the aid of methods of the CFD for accurate assessment of dynamic effects between the vehicle and the external sea water environment. The vehicles are inertia propelled, i.e. move due to mass or configuration of mass

© Copyright by Łukasiewicz Research Network – Institute of Aviation

change, or hybrid propelled, i.e. using inertia and engines to move. The steady state gliding motion is defined by Zhang et al., 2012, as: "for a particular change in buoyancy and fixed position of moving mass, the state variables of the glider remain unchanged and angular velocity remains zero for its sawtooth gliding motion".

The paper focuses on AUV inertia based propelled, i.e. not equipped with thrusters or hybrid ones, equipped additionally with thrusters. AUVs are then a class of underwater vehicles not equipped with external propulsion systems. There are quite a lot of types of such AUVs currently available such as Slocum [1], Spray [2] or Sea-glider [3]. They are designed for long range missions, consume small energy, are low cost and of significant endurance. They can be applied in oceanography, in rescue and cleaning sea missions. Their method of propulsion relies upon changing their buoyancy with internal pumping systems enabling them up and down motions, and their forward gliding motions are generated by hydrodynamic lift forces exerted on a pair of wings attached to a glider hull. The resulting AUV motion is a "saw-tooth motion" pattern in the vertical plane and a straight line motion in the horizontal plane. Low energy and easy propulsion has enabled for AUV various mission designs in real applications, where either a single glider or a group were used, see e.g. [4, 5]. The other method of propulsion for an AUV is by using a movable internal mass. Such models were derived in e.g. [6, 7]. Other kind of motion of an AUV derived and reported in references is along a spiral curve (see the description in [8]). The spiral motion can be obtained by rotating an internal mass, (e.g., the battery pack), or a rudder attached to the tail section of the glider.

2. TEST SETUP AND METHODOLOGY

As an ingredient of a mathematical description of an AUV dynamics, an adequate model of hydrodynamic interactions is utterly important. In late 60's, Gertler and Hagen [9] proposed completely analytical yet quite complex set of formulas for hydrodynamic force and moment components in the body-fixed reference frame, which are reminiscent of expressions used in the flight dynamics. Most recently, the CFD methods have become increasingly popular in hydromechanical modelling of AUVs. The RANS-based simulations were used to help calibration of the coefficient-based models [10, 11] or to provide steady-state hydrodynamic characteristics for such models [12-14]. Different turbulence models applied to RANS simulations of flows past a drifting submarine were investigated and compared in [15]. In a similar work [16], the RANS simulations were used to calculate flow and forces past a submarine performing steady turns.

The most advanced usage of the CFD method consists in solving the full set of equations for unsteady turbulent flow (URANS model) simultaneously, i.e. fully coupled with the equations of motion. It means that either the flow equations need to be solved in a domain which changes in time in a priori unknown way or the flow problem needs to be posed and solved in the body-fixed non-inertial reference frame. In the latter case, the far-field conditions become time-dependent and non-uniform. Yet another approach to the CFD-based determination of the hydrodynamic loads is presented in [17]. In this work, a computational domain is divided into two parts: the internal part surrounding the submarine and the "far-field" part around. Each part has been meshed independently. The whole domain moves linearly with instantaneous velocity of the submarine but only the internal mesh performs rotary motion following the spatial orientation of the vehicle. This way, the problem of deforming meshes is replaced by the interpolation problem at the interface of sliding meshes. The accuracy of force prediction is very good. In this study Commercial CFD solver ANSYS Fluent 18.2 was used to solve the steady state Reynolds averaged Navier Stokes (RANS) equations. The Shear Stress Transport (SST) $k - \omega$ model is chosen for turbulence model, which is widely used in flow separation problems and likely to be found at the aft of the AUV.

2.1. Geometry

Geometry of the AUV was created in ANSYS SpaceClaim 2017 and was designed based on the glider in the paper [18] for the possibility of comparing the results. The sister glider was the background for our research. Our glider called "Hulke" has a torpedo shaped hull with tail shapes and fixed wings, elevator and rudder. Torpedo type hull is a cylindrical body with a large ratio between the length and diameter, L/D = 9.76. This shape provides good features and is widespread used by all major manufacturers of AUVs. The vehicle presented in Figure 1 is symmetrical along the XZ plane, for this reason the calculation were performed for the half of the body to save the calculation costs.

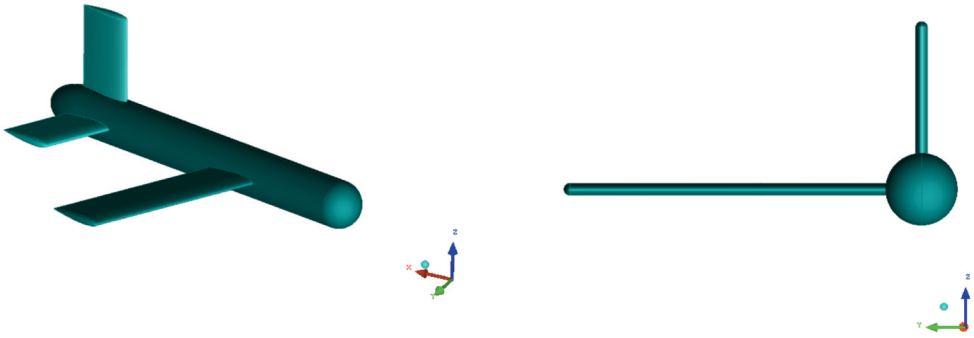

Figure 1. The geometry of "Hulke"

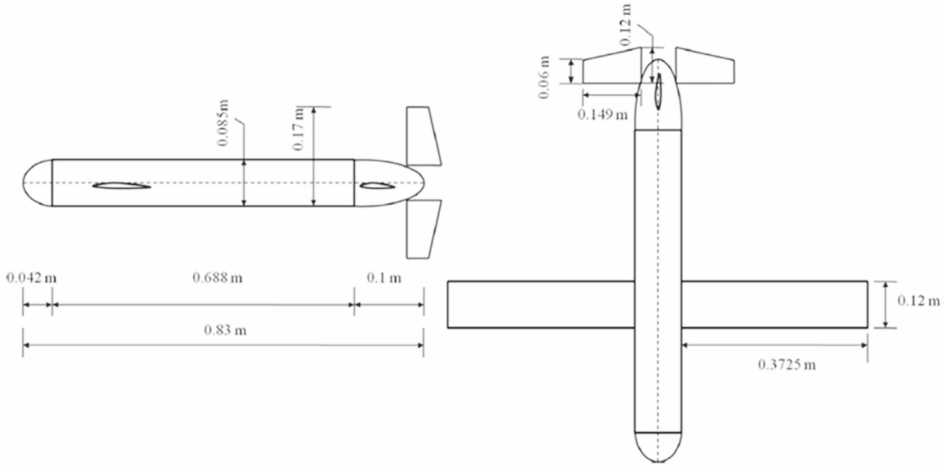

Figure 2. Dimensions of the sister glider, Alex [20]

To model the profiles of the bow and stern of the vehicle *Myring Equations* are commonly used. These theoretical equations describe curves for bow and stern of torpedo bodies which generate the smallest possible drag coefficient [21]. The equations are as follows:

- Bow

$$r_1(x) = \frac{1}{2} D \left[1 - \left(\frac{x-a}{a} \right)^2 \right]^{1/n} \tag{1}$$

- Stern

$$r_2(x) = \frac{1}{2}D - \left[\frac{3D}{2c^2} - \frac{tg\theta}{c}\right](x-a-b)^2 + \left[\frac{D}{c^3} - \frac{tg\theta}{c^2}\right](x-a-b)^3 \quad (2)$$

where all parameters of the equations are geometric (except parameter *n*) and are shown in Figure 3. These equations allowed to validate the studied geometry according to the optimal hydrodynamic shape.

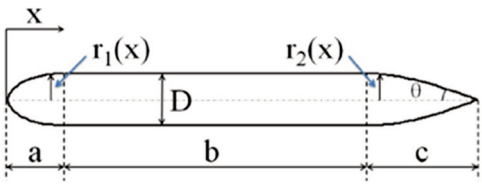

Figure. 3. Schematic figure of the AUV hull and geometric parameters of *Myring Equations* [21]

Table 1. "Hulke" geometric parameters used in the simulations

Parameter	Value (m)
a	0.042
b	0.688
c	0.1
D	0.085

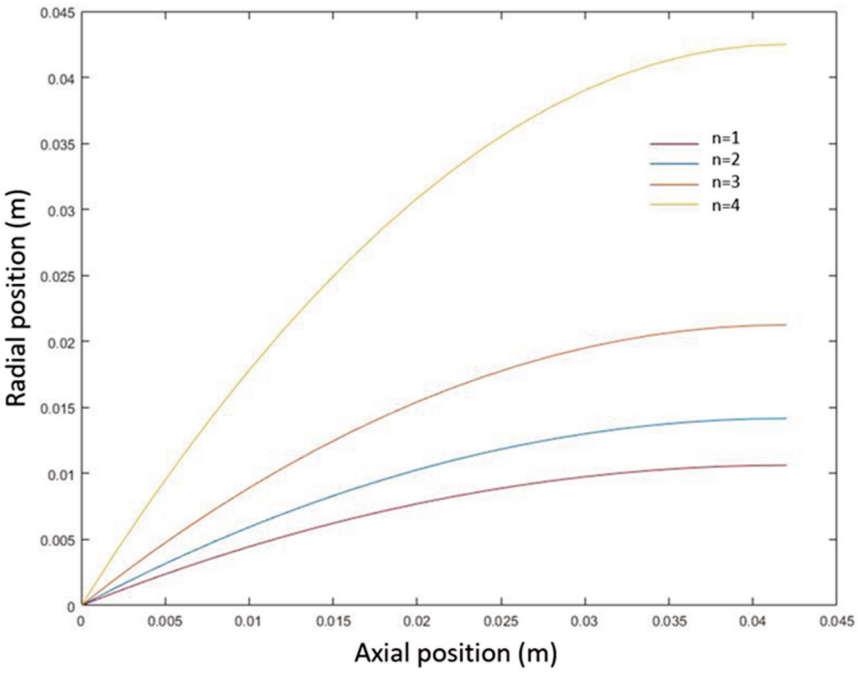

Figure 4. Bow profiles analyzed for different parameters n

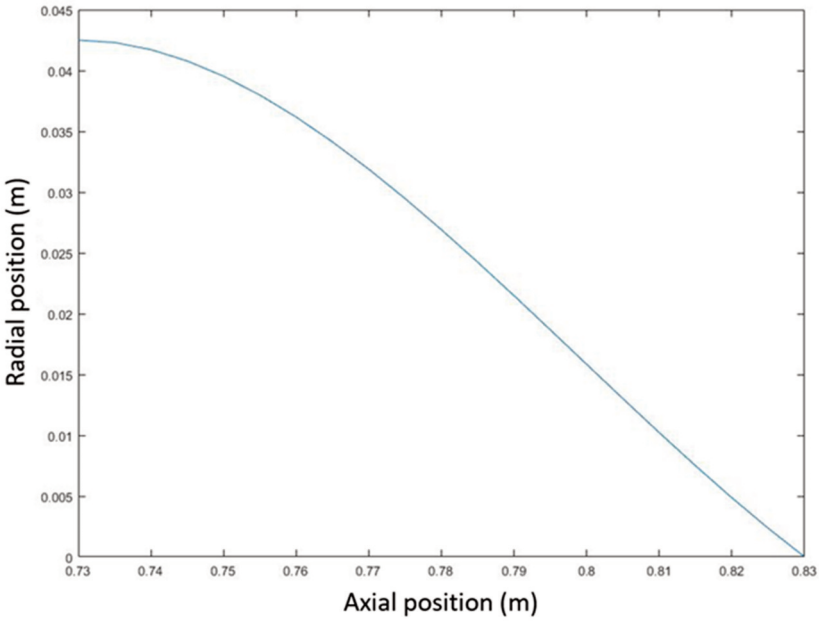

Figure 5. Stern profile for θ=25°

Myring equations shows that the bow of studied glider is well fitted if n=3, but the stern should be improved to get optimal hydrodynamic shape. Higher length to diameter ratio (L/D) was desirable for a glider. The predicted value of $L / D \approx 9$ was considered sufficiently high. Results in the literature [18] showed that the symmetrical wing profile performs better than the cambered wing profile. Therefore, NACA0012 profile was adopted for the glider.

2.2. CFD Analysis

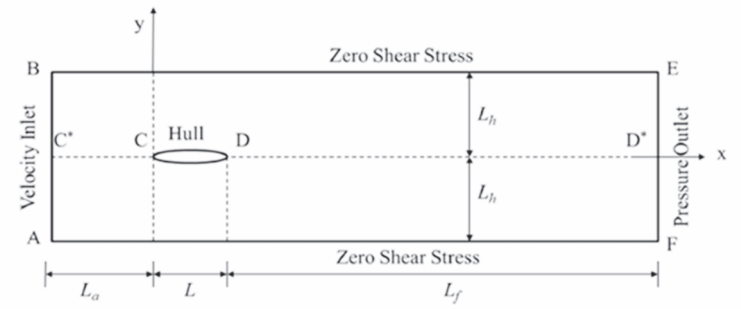

Figure 6. Computational domain for glider with boundary conditions [18]

Studied glider was assigned for the Baltic Sea mission, therefore the maximum operational depth is 25 m, where the absolute pressure is around 3500 hPa. According to the [22], the density of the water in the Baltic Sea at the 10°C is ρ=1005 kg/m^3 and dynamic viscosity is μ=1.33e-3 kg/ms.

ITTC [21] recommendations for marine CFD applications specify that the computational domain around the experimental glider shown in Figure 6 should extends L_a (= 1.3 L) in the upstream of the leading edge of the body, L_h (= 1.3 L) in the radial direction (from the centerline of the body) and

L_f(= 5 L) in the downstream of the trailing edge of the body. These dimensions of the domain were studied, however, the interaction between fluid and hull was noticed on the upper and bottom wall. The distribution of pressure and velocity in the cross-section (passing through the vehicle) was investigated; the pressure gradient caused by the presence of the glider was noticeable at the end of the domain. The recommended domain dimensions do not work with different angles of attack. Due to that reason the domain was scaled by the XYZ product factor = 3.

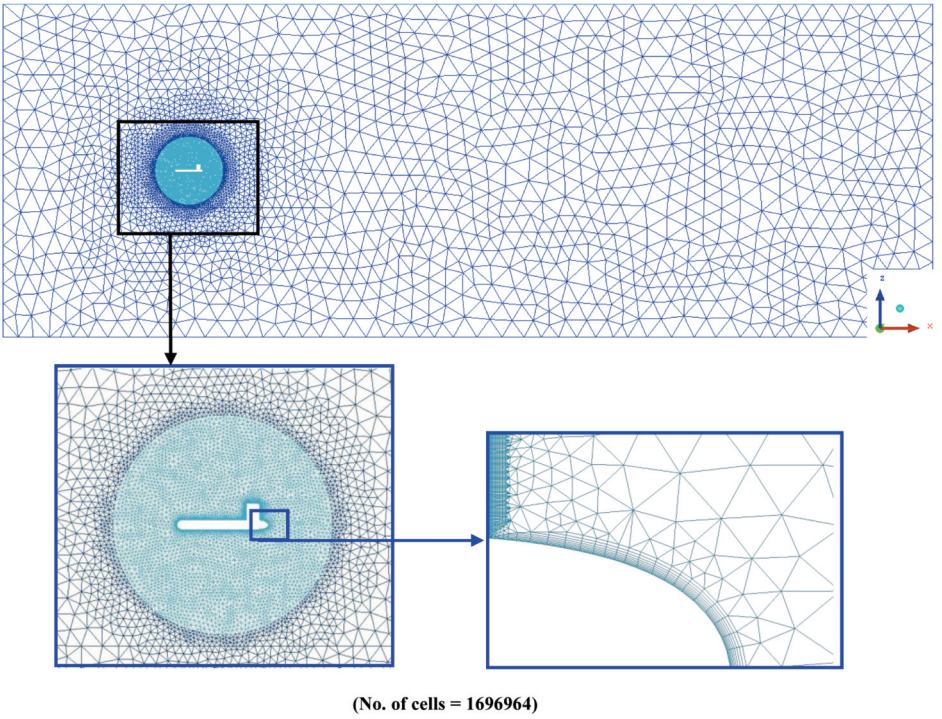

Figure 7. Distribution of the cell around 3D model of the underwater glider

The domain around the body was discretized with the unstructured mesh. The volume tetra mesh was created by the Robust (Octree) method. The mesh should be dense in areas where the flow velocities are sensitive to grid spacing and coarse in other areas. Due to that reason the region around the hull was concentrated. 10 prism layer was sufficient to perform flow characteristics in the boundary layer, Figure 7. The thickness of boundary layer was set according to the ITTC, CFD marine recommendation [19]:

$$\delta = 0.035\, L \cdot \mathrm{Re}^{-1/7} \tag{3}$$

where:
L – the length of the glider [m],

Re – Reynolds number $\mathrm{Re} = \dfrac{v \cdot L}{\vartheta}$, (v – velocity of the glider [m/s]; υ – kinematic viscosity [m²/s]),

Re = 3e5.

Relying on [19], the non-dimensional wall distance can be defined in terms of Reynolds number in the following way:

$$\frac{y}{Lpp} = \frac{y^{+}}{\mathrm{Re}\sqrt{Cf/2}} \tag{4}$$

where:
y – is the first required cell height and C_f is an estimate of the skin friction coefficient, based on the ITTC standard method.

$$C_f = 0.075/\left(\log_{10}\mathrm{Re} - 2\right)^2 \tag{5}$$

$C_f = 0.0063$ [-]
$y^+ = 2.4$ [-].

CFD calculations presents similar values for average $y^+ = 2.1$ (at zero alpha angle). Figure 8 below presents dimensionless wall distance parameter distribution calculated in ANSYS Fluent R18.2.

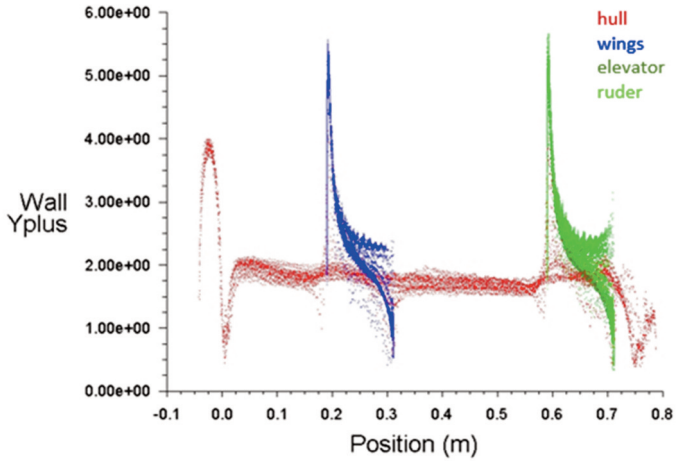

Figure 8. Wall distance parameter distribution from Fluent

Commercial CFD solver ANSYS Fluent 18.2 has been used to solve the steady state Reynolds averaged Navier Stokes (RANS) equations. The Shear Stress Transport (SST) k − ω model was chosen for turbulence model, which is widely used in flow separation problems and likely to be found at the aft of the AUV.

The convergence is decided by the standard deviation of the viscous pressure resistance coefficient and frictional resistance coefficient displayed in per cent of the average force. The convergence criterion in the present study was set as 1% for the viscous pressure resistance coefficient and frictional resistance coefficient. Computations are carried out until steady state is reached [20].

Glider was tested for the constant velocity 0.5 m/s and range of angle of attack (α = −8° to 8° in steps of 2°), the drag and lift coefficients are computed using CFD (calculated for the front reference surface) and compared with CFD results presented in Yogang Singh et al. [18]. The results for drag characteristics are similar, but bigger differences are noticed in the lift coefficients, probably because of the different NACA profile used.

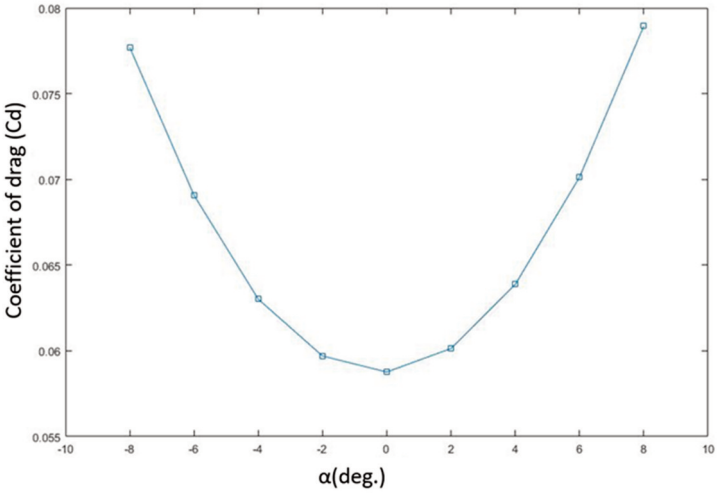

Figure 9. Drag coefficient (Cd) as function of angle of attack α: CFD results

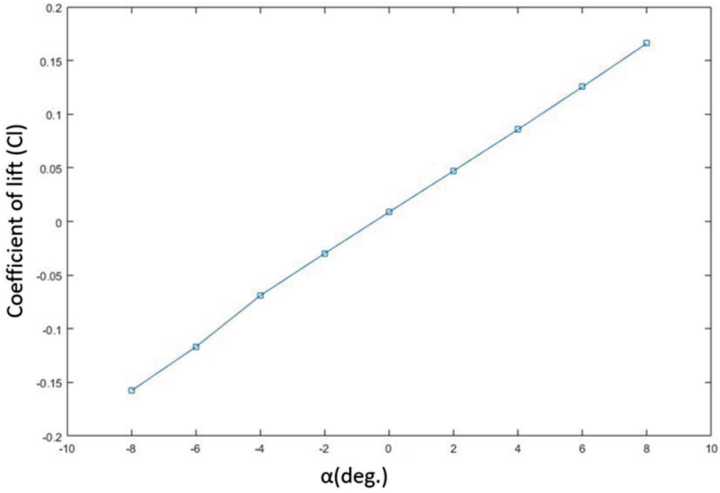

Figure 10. Lift coefficient (Cl) as function of angle of attack α: CFD results

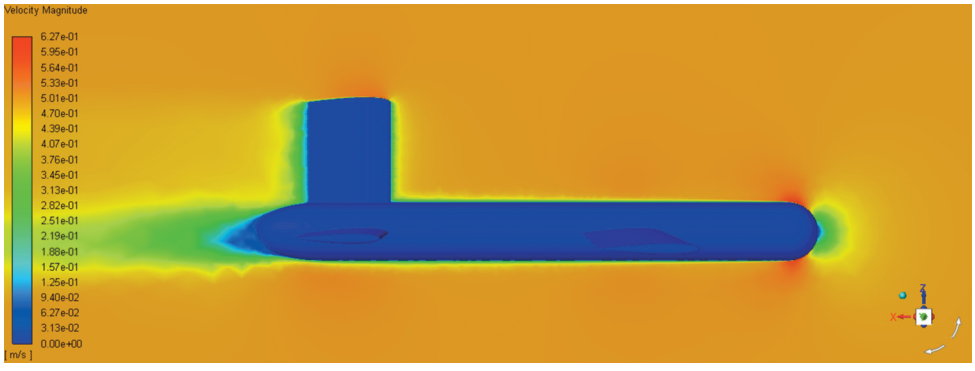

Figure 11. Velocity magnitude around the glider body, V=0.5 m/s, angle of attack = 0°. X0Z geometry plane

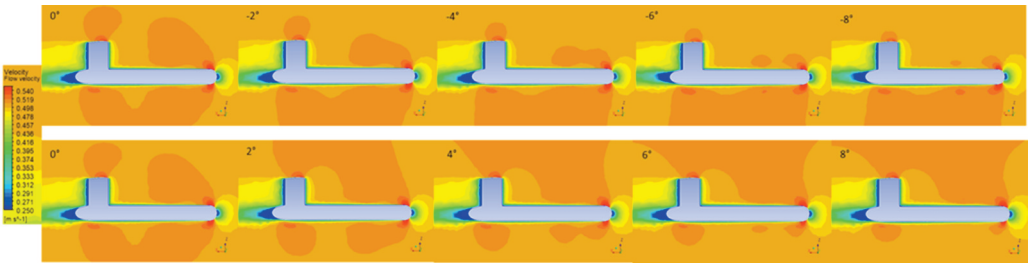

Figure 12. Velocity magnitude around the glider body. V=0.5 m/s, angle of attack varying from -8 to 8°. X0Z geometry plane

3. MATHEMATICAL APPROACH OF GLIDER MOTION IN VERTICAL PLANE

This chapter presents the correlation between inertial coordinate system and body-related system. The chapter mentioned about the forces and moments acting on AUV. The force coefficients such as lift and drag coefficient from CFD are taken into consideration while equation of motion are solved. In the AUV model the forces are resolved into axial and normal forces. The origin of inertial system, E-frame, was taken at the free surface, so depth was along Z axis. Equations of motion are defined in B-frame. CB was located at the center of the ellipsoidal hull (origin of B-frame). The CG was located slightly offset from CB along axial direction to create a constant gravitational moment. The velocity of the glider along x, y and z – axis was represented by U, V and W respectively while the angular velocity of the glider along x, y and z – axis was represented by P, Q and R, respectively, all in B-frame.

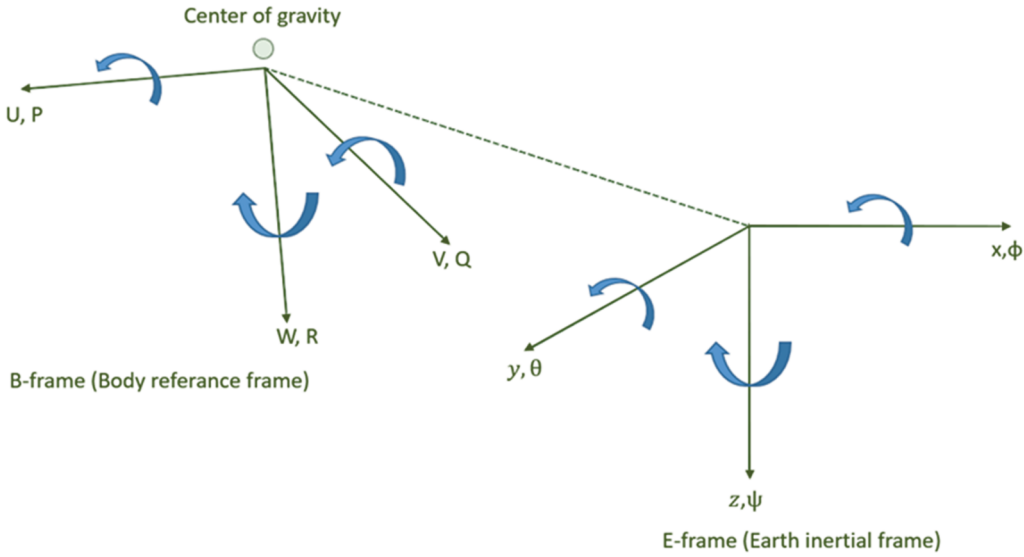

Figure 13. Body and Earth reference frames

Vectors of linear and angular velocities (V_0 and Ω respectively) in the system related to the glider (B-frame) can be presented as:
– vector of the instantaneous linear velocity V_0, where the coordinates are:

U, V, W: $V_0 = Ui + Vj + Wk$ – instantaneous velocity.

– vector of the instantaneous angular velocity Ω, where the coordinates are:

P (roll velocity), Q (pitch velocity), R (yaw velocity): $\Omega = Pi + Qj + Rk$ – angular velocity.

The coordinates of the linear velocity measured in the inertial system (i.e. E-frame): $\dot{x}, \dot{y}, \dot{z}$ are related to the coordinates U, V, W through the transformation matrix. Such a relation can be written with the matrix equation as follows:

$$\begin{bmatrix} U \\ V \\ W \end{bmatrix} = \Lambda_v \begin{bmatrix} \dot{x} \\ \dot{y} \\ \dot{z} \end{bmatrix} \tag{6}$$

The transformation matrix was obtained by successively rotating the coordinate system around the respective axes by the following angles: ψ, θ, ϕ and projection of velocity vectors.

- system O x_1 y_1 z_1 is rotated by an angle ψ around the axis O z_1
- system O x_2 y_2 z_2 is rotated by an angle θ around the axis O y_2
- system O x_3 y_3 z_3 is rotated by an angle ϕ around the axis O x_3

The result of the first operation, i.e. the rotation by an angle ψ, around Oz_1 axis, following equations were obtained:

$$\begin{aligned} U_2 &= \dot{x}_1 \cos\psi + \dot{y}_1 \sin\psi \\ V_2 &= -\dot{x}_1 \sin\psi + \dot{y}_1 \cos\psi \\ W_2 &= \dot{z}_1 \end{aligned} \tag{7}$$

In the next step, the rotation was made around the y_2 axis by an angle θ. As a result of this turnover, the following relationships were obtained:

$$\begin{aligned} U_3 &= U_2 \cos\theta - \dot{y}_1 \sin\theta \\ V_3 &= V_2 \\ W_2 &= U_2 \sin\theta + W_2 \cos\theta \end{aligned} \tag{8}$$

When rotating around the z_3 axis by an angle ϕ, we get:

$$\begin{aligned} U &= U_3 \\ V &= V_3 \cos\phi + W_3 \sin\phi \\ W &= -V_3 \sin\phi + \cos\phi \end{aligned} \tag{9}$$

As a result of three operations (around each axis), the following transformation matrix Λ_v was created (this is the product of three matrices representing a rotation around a given axis):

$$\Lambda_v = \begin{bmatrix} \cos\theta\cos\psi & \cos\theta\sin\psi & -\sin\theta \\ \sin\phi\sin\theta\cos\psi - \cos\phi\sin\psi & \sin\phi\sin\theta\sin\psi + \cos\phi\cos\psi & \sin\phi\cos\theta \\ \cos\phi\sin\theta\cos\psi + \sin\phi\sin\psi & \cos\phi\sin\theta\sin\psi - \sin\phi\cos\psi & \cos\phi\cos\theta \end{bmatrix} \quad (10)$$

In order to determine the velocity coordinates $\dot{x}, \dot{y}, \dot{z}$ in the inertial system, the following matrix equation should be solved:

$$\begin{bmatrix} \dot{x} \\ \dot{y} \\ \dot{z} \end{bmatrix} = \Lambda_v^{-1} \begin{bmatrix} U \\ V \\ W \end{bmatrix} \quad (11)$$

The matrix inverse to the transformation matrix was calculated using the MatLab program.
In the case of angular velocity and its P, Q, R coordinates, the process of determining the transformation matrix was analogous to the process that has been described above, but the transformation matrix was much simpler. The equation describing this relationship is as follows:

$$\begin{bmatrix} P \\ Q \\ R \end{bmatrix} = \Lambda_\Omega \begin{bmatrix} \dot{\phi} \\ \dot{\theta} \\ \dot{\psi} \end{bmatrix} \quad (12)$$

And the transformation matrix after transformations looks as follows:

$$\Lambda_\Omega = \begin{bmatrix} 1 & 0 & -\sin\theta \\ 0 & \cos\phi & \sin\phi\cos\theta \\ 0 & -\sin\phi & \cos\phi\cos\theta \end{bmatrix} \quad (13)$$

The determination of angular velocities in the inertial system wass the result of the solution:

$$\begin{bmatrix} \dot{\phi} \\ \dot{\theta} \\ \dot{\psi} \end{bmatrix} = \Lambda_\Omega^{-1} \begin{bmatrix} P \\ Q \\ R \end{bmatrix} \quad (14)$$

In the studied case, angles and velocities are relatively small. The angles ϕ, θ, ψ are particulary important, because at $\theta=\pm 90°$ a singularity would occur when reversing the transformation matrix, then Quasi-Euler angles should be replaced by an alternate kinematic representation such as quaternions or Rodriguez parameters. In the examined case the angles do not reach such values (the assumption arises from the speed and the way of vehicle movement).

Finally, equations can be summarized in the following form:

$$\begin{aligned}
\dot{x} &= U\cos\psi\cos\phi + V\left(\cos\psi\sin\theta\sin\phi - \sin\psi\cos\phi\right) + W\left(\cos\psi\sin\theta\sin\phi + \sin\psi\sin\phi\right)\\
\dot{y} &= U\sin\psi\cos\phi + V\left(\sin\psi\sin\theta\sin\phi + \cos\psi\cos\phi\right) + W\left(\sin\psi\sin\theta\cos\phi - \cos\psi\sin\phi\right)\\
\dot{z} &= -U\sin\theta + V\cos\theta\sin\phi + W\cos\theta\sin\phi\\
\dot{\phi} &= P + Q\sin\phi\ \mathrm{tg}\theta - R\cos\phi\ \mathrm{tg}\theta\\
\dot{\theta} &= Q\cos\phi - R\sin\phi\\
\dot{\psi} &= \left(Q\sin\phi + R\cos\phi\right)\frac{1}{\cos\theta} \equiv \sec\theta\left(Q\sin\phi + R\cos\theta\right)
\end{aligned} \tag{15}$$

P, Q, R, U, V, W are quasi velocities.

3.1. Forces and moments acting on AUV

In order to model the AUV movement properly, external forces and moments acting on the glider should be taken into account. External loads are presented in the form of two vectors whose coordinates are associated with the vehicle, i.e. the system O_{xyz}. Forces are represented by the vector F with components X, Y, Z. The force vector was as follows:

$F = Xi + Yj + Zk$ − vector of external forces.

where: X is longitudinal force, Y lateral force and Z is a vertical force.

The vector of vehicle loading moments can be described by the three components *L, M, N*. Vector of hydrodynamic moments:

$M = Li + Mj + Nk$ − the moment vector.

The corresponding coordinates are L − rolling moment, M − pitching moment, and N − yawing moment. Finally, equations can be summarized in matrix form as follows:

$$\begin{aligned}
&m\left[\dot{U} - VR + WQ - x_g\left(Q^2 + R^2\right) + z_g\left(PR + \dot{Q}\right)\right] = \sum X_{ext}\\
&m\left[\dot{V} - WP + UR + z_g\left(QR - \dot{P}\right) + x_g\left(QP + \dot{R}\right)\right] = \sum Y_{ext}\\
&m\left[\dot{W} - UQ + VP - z_g\left(P^2 + Q^2\right) + x_g\left(RP + \dot{P}\right)\right] = \sum Z_{ext}\\
&I_{xx}\dot{P} + \left(I_{zz} - I_{yy}\right)QR + m\left[-z_g\left(\dot{V} - WP + UR\right)\right] = \sum L_{ext}\\
&I_{yy}\dot{Q} + \left(I_{xx} - I_{zz}\right)RP + m\left[z_g\left(\dot{U} - VR + WQ\right) - x_g\left(\dot{W} - UQ + VP\right)\right] = \sum M_{ext}\\
&I_{zz}\dot{R} + \left(I_{yy} - I_{xx}\right)PQ + m\left[x_g\left(\dot{V} - WP + UR\right)\right] = \sum N_{ext}
\end{aligned} \tag{16}$$

where: I_{xx}, I_{yy}, I_{zz} are the moments of inertia;

Right side of above equations, hides hydrostatic, hydrodynamic, lift, added mass and propeller force. Values of individual forces and moments might be calculated by the CFD or obtained from experimental tests. In this paper only hydrodynamic and lift forces were considered. Having the external forces and moments, equations of motions for the glider in six degrees of freedom can be calculated. MatLab solves nonstiff differential equations using different numerical methods. The most popular solvers are ODE45 and ODE113. The first allows solving the system of equations, assuming the standard calculation error for MatLab. In the case when very accurate solutions are needed and the ODE45 cannot cope with calculations, the ODE113 solver is chosen.

4. CONCLUSIONS

In this paper the hydrodynamic single-phase flow around the underwater glider hull was discussed. The study was related to sea water flow in the turbulent regime by using the ANSYS Fluent R18.2 commercial software. The results show the proper tendency in hydrodynamic characteristic as a function of angle of attack. Furthermore, the results were compared with results presented in the literature [18]. Other forces such as added mass and propeller force need to be considered in the future. This work will contribute to dynamic modeling and three-dimensional motion simulation of a torpedo shaped underwater glider. The force coefficients of lift and drag taken from the CFD are used to solve equation of glider motion.

BIBLIOGRAPHY

[1] Webb D.C., Simonetti P.J., Jones C.P. SLOCUM, an underwater glider propelled by environmental energy. IEEE J. Oceanic Eng. 2001, 26 (4), 447-452.

[2] Sherman J., Davis R.E., Owens W.B., Valdes J., 2001. The autonomous underwater glider "spray". IEEE J. Oceanic Eng. 26 (4), 437-446.

[3] Eriksen C.C., Osse T.J., Light R.D., Wen,T., Lehman T.W., Sabin P.L., Ballard J.W., Chiodi A.M., 2001. Sea-glider: a long range autonomous underwater vehicle for oceanographic research. IEEE J. Oceanic Eng. 26 (4), 424-436.

[4] Zhang F., Fratantoni D.M., Paley, D., Lund J., Leonard N.E., Control of coordinated patterns for ocean sampling. Int. J. Control, 2007, 80 (7), 1186-1199.

[5] Leonard N.E., Paley D.A., Davis R.E., Fratantoni D.M., Lekien F., Zhang F., Coordinated control of an underwater glider fleet in an adaptive ocean sampling field experiment in Monterey bay. J. Field Robot. 2010, 27 (6), 718-740.

[6] Graver J., Leonard N.E., Underwater glider dynamics and control. In: 12th International Symposium on Unmanned Untethered Submersible Technology, Durham, 2001, 1-14.

[7] Bhatta P., Leonard N.E., Nonlinear gliding stability and control for vehicles with hydrodynamic forcing. Automatica, 2008, 44 (5), 1240-1250.

[8] S. Zhang, J. Yu, A. Zhang, F. Zhang, Spiraling motion of underwater gliders: Modeling,analysis, and experimental results, Ocean Engineering, 2013, 60, 1-13

[9] Gertler M., Hagen G.R., Standard equations of motion for submarine simulation, Report 2510, Naval Ship Research and Development Center, June 1967.

[10] Yumin Su, Jinxin Zhao, Jian Cao and Guocheng Zhang, Dynamics modeling and simulation of autonomous underwater vehicles with appendages. J. Marine Sci. Appl. 2013, 12, 45-51.

[11] de Barros E.A., Pascoal A., de Sa E., Investigation of a method for predicting AUV derivatives. Ocean Engineering, 2008, 35, 1627-1636.

[12] Isa K., Arshad M.R., Ishak S., A hybrid-driven underwater glider model, hydrodynamics estimation, and an analysis of the motion control. Ocean Engineering, 2014, 81, 111-129.

[13] Fang Liu, Yanhui Wang, Wendong Niu, Zhesong Ma, and Yuhong Liu: Hydrodynamic performance analysis and experiments of a hybrid underwater glider with different layout of wings. IEEE, 978-1-4799-3646-5/14, 2014.
[14] Singh Y., Bhattacharyya S.K., Idichandy V.G., CFD approach to steady state analysis of an underwater glider. IEEE, 978-1-4799-4918-2/14/, 2014.
[15] Phillips A. B., Turnock S. R., Furlong M., Influence of turbulence closure models on the vortical flow field around a submarine body undergoing steady drift, J. Marine Sci. Techn., 2010, 15(3), 201-217.
[16] Zhang J.T. Jordan A. M., Gerber,A. G., Gordon A., Holloway L., Watt, G.D., Simulation of the flow over axisymmetric submarine hulls in steady turning, Ocean Engineering, 2013, 57, 180-196. 2014, 102, 215-236.
[17] Xiaocui W., Yiwei W., Chenguang H., Zhiqiang H., Ruiwen Y., An effective CFD approach for marine-vehicle maneuvering simulation based on the hybrid reference frames method. Ocean Engineering, 2015, 109, 83-92.
[18] Yogang Singh ∗, S.K. Bhattacharyya, V.G. Idichandy, CFD approach to modelling, hydrodynamic analysis and motion characteristics of a laboratory underwater glider with experimental results, Journal of Ocean Engineering and Science 2 (2017) 90-119.
[19] ITTC, Recommended procedures and guidelines: practical guidelines for ship CFD applications, 7.5, ITTC, 2011, pp. 1-18.
[20] Ichihashi N., Ikebuchi T., Arima M., in: Proceedings of the eighteenth ISOPE conference, ISOPE 2008, Canada, 2008, pp. 156-161. ISBN: 1-880653-68-0.
[21] Myring D.F. (1976) A Theoretical Study of Body Drag in Subcritical Axisymmetric Flow. The Aeronautical Quarterly, 27, 186-194.
[22] Lepparanta M., Myrberg K., Physical oceanography of the Baltic Sea, Praxis Publishing Ltd, Chichester, UK, 2009, ISBN 978-3-540-79702-9.

MODELOWANIE CHARAKTERYSTYK HYDRODYNAMICZNYCH PODWODNEGO SZYBOWCA Z UŻYCIEM METOD NUMERYCZNEJ MECHANIKI PŁYNÓW

Streszczenie

Autonomiczne podwodne szybowce to pojazdy napędzane wypornością i siłą nośną. Ruch glidera w stanie ustalonym jest ruchem „piłokształtnym". Sposób napędu polega na zmianie ich wyporności za pomocą wewnętrznego systemu pomp, umożliwiającego im nurkowanie lub wynurzanie się z wody, a ich ruchy w przód są generowane przez hydrodynamiczne siły nośne wywierane na parę skrzydeł przymocowanych do kadłuba. W ramach tej pracy wyznaczono charakterystykę siły oporu i siły nośnej szybowca z zastosowaniem metod Numerycznej Mechaniki Płynów, wyniki porównano z innymi danymi z literatury. Charakterystykę przepływu, rozkład siły nośnej i oporu przy różnych kątach pochylenia badano dla liczb Reynoldsa o wartości około 105 dla konfiguracji skrzydeł NACA0012. Zmiennym parametrem szybowca jest kąt pochylenia, prędkość przepływu była stała i wynosiła 0,5 m/s. Kąt pochylenia kadłuba zmieniał się od -8° do 8° z krokiem 2°. Wyniki z CFD są wykorzystywane do obliczania równań ruchów szybowca w płaszczyźnie pionowej. W niniejszej pracy została rozpatrzona hydrodynamika i generowane siły nośne. Równania ruchu będą rozwiązywane w oprogramowaniu MatLab. Praca ta przyczyni się do stworzenia odpowiedniego modelu dynamiki szybowca podwodnego.

Słowa kluczowe: AUV, CFD, opór hydrodynamiczny, szybowiec, glider, podwodny szybowiec.